Proceedings World Geothermal Congress 2026
Calgary, Canada, June 8 – 11, 2026

Comparison of Landsat 8 Level 2 Land Surface Temperature with Shallow Ground Thermal Measurements in Barren Crater Settings

Suryantini[1,2,3]* and Hendro Wibowo[2]

Applied Geology Research Group, Faculty of Earth Sciences and Technology (FITB) , Institut Teknologi Bandung (ITB), Indonesia[1]*, Undergraduate Program in Geological Engineering, Faculty of Earth Sciences and Technology (FITB) , Institut Teknologi Bandung (ITB), Indonesia[2], Geothermal Master Program, Faculty of Mining and Petroleum Engineering (FTTM), Institut Teknologi Bandung (ITB), Indonesia[3]

suryantini@itb.ac.id

Keywords: Land Surface Temperature (LST), geothermal exploration, Landsat 8/9, SWIR alteration indices, clay index, silica index, surface thermal anomalies, Kawah Domas, Indonesia

ABSTRACT

The objective of this study is to evaluate the relationship between satellite-derived Land Surface Temperature (LST) from Landsat 8 Level-2 data and shallow ground temperature measurements in a geothermal crater setting, and to assess how integrating LST with SWIR-based clay and silica alteration indices can improve the identification of surface thermal and mineralogical anomalies for geothermal exploration. This study compares Landsat 8 Level-2 LST with shallow ground temperatures (25–50 cm depth) in the Kawah Domas crater area, West Java, Indonesia, and integrates SWIR-based alteration indices for clay and silica to assess surface mineralogy. Although the quantitative agreement between LST and ground temperature measurements is limited, the spatial alignment of elevated LST zones with areas characterized by lower clay index and higher silica index values demonstrates a strong correspondence between surface thermal anomalies and underlying alteration patterns. The results demonstrate that, despite spatial resolution limitations, combining LST with SWIR-derived mineral indices maximizes the information obtainable at the exploration stage. This approach provides a practical framework for identifying promising geothermal zones and guiding subsequent field investigations.

1 INTRODUCTION

Satellite-derived LST has been widely applied in geothermal exploration to indicate hydrothermal activity, fault-controlled upflow zones, or shallow conductive anomalies. Its main advantage lies in cost-effectiveness and wide-area reconnaissance capability.

Several studies have demonstrated its potential for geothermal mapping in Indonesia (Dewanto et al., 2025; Fathya et al., 2023; Hidayat et al., 2023; Nugraha et al., 2021; Augusty et al., 2022). This paper investigates the relationship between Landsat-derived LST and shallow ground temperature measurements at Kawah Domas crater. The aim is to assess whether visual spatial agreement—despite numerical mismatch—can still provide meaningful geothermal interpretation.

2 DATA AND METHODS

2.1 Study Area

The study area (Figure 1 left) is located at Kawah Domas, Mount Tangkuban Parahu, West Java, Indonesia. The site is characterized by active steam vents and NE–SW fault structures. It covers approximately 6 hectares with elevation ranging from 1550 to 1650 m a.s.l. The terrain consists of altered volcanic deposits with minimal vegetation (Figure 1 right).

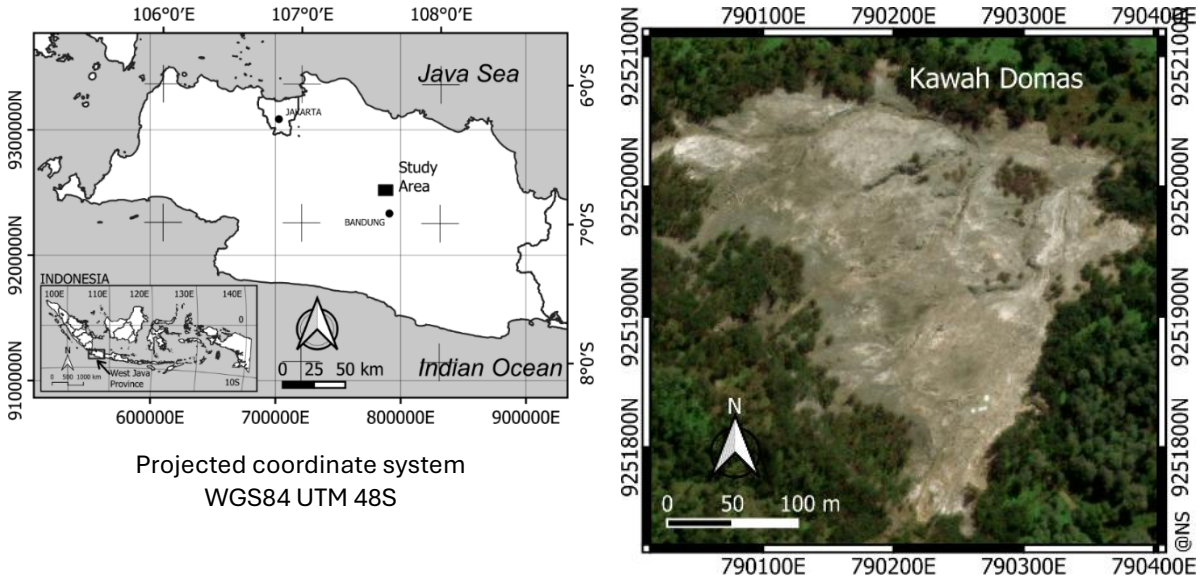


Figure 1. Study area (left), and Kawah Domas (right).

2.2 Data

Two datasets were used: (1) shallow ground temperature measurements acquired between May–June 2012, and (2) Landsat 8 Collection 2 Level-2 LST acquired on May 13, 2016

Ground temperature was measured using an auger at depths of 25–50 cm (Figure 2). The Landsat 8 Level-2 data (U.S. Geological Survey, 2023) provide atmospherically corrected surface reflectance and temperature products generated using LaSRC and single-channel algorithms. These data are CEOS Analysis Ready Data (ARD), ensuring minimal preprocessing requirements and interoperability across time and sensors. Landsat scene selection was carried out by identifying manually all available clear-sky Landsat 8 and 9 Level-2 scenes covering the study area from the USGS EarthExplorer database (https://earthexplorer.usgs.gov/), yielding 57 candidate scenes. The scene acquired on 13 May 2016 was chosen for analysis as it was the closest in acquisition date to the period of shallow ground temperature measurements.

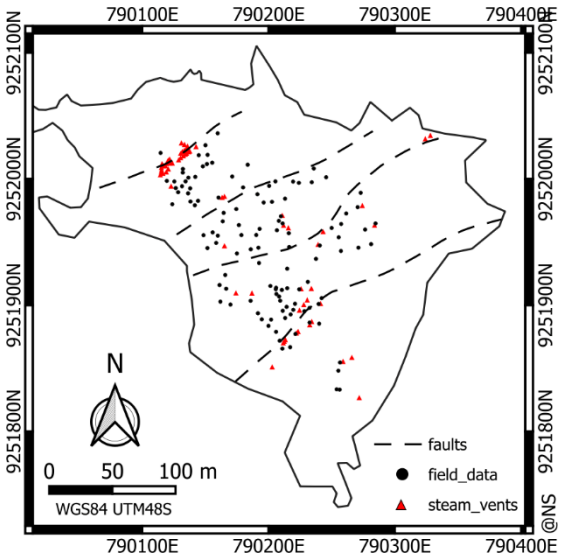


Figure 2. Ground temperature measurement locations.

2.3 Data Processing

Landsat scenes were projected to WGS84 UTM Zone 48S. The spatial resolution of Landsat LST in the USGS Collection 2 Level-2 product is 30 m (resampled from its original 100 m TIR band). The field temperature map was interpolated from point measurements using kriging method, and subsequently downscaled to the same spatial resolution as the Landsat LST using bilinear resampling to enable pixel-to-pixel comparison.

In addition to LST, SWIR-based alteration indices were computed from the Landsat surface reflectance bands to characterize clay and silica distribution:

- Clay Alteration Index (Ninomiya, 2003):

$$Clay\ Alteration\ Index = \frac{(SWIR1 - SWIR2)}{(SWIR1 + SWIR2)}$$

  Where: SWIR1 = Shortwave-Infrared band (1547–1749 nm), SWIR2 = Shortwave-Infrared band (2064–2345 nm).

- Silica index (Sabins, 1999):

$$Silica\ Index = \frac{(SWIR1 - NIR)}{(SWIR1 + NIR)}$$

  Where: NIR = Near-Infrared band (772–898 nm).

LST values corresponding to downscaled ground-measurement raster (30 m pixel) locations were extracted for regression analysis. In addition, a temperature-difference map (LST – Ground) was generated to evaluate the magnitude and spatial distribution of discrepancies between field and satellite temperatures.

Visualization included:

1. Side-by-side thermal maps of LST and downscaled ground measurements.
2. Scatterplots with linear regression between LST and ground temperature.
3. Paired display of downscaled ground-temperature and temperature-difference maps for spatial comparison.
4. Maps of clay and silica indices to assess alteration patterns and potential correlations with temperature anomalies.

2.4 Analysis

Correlation (R^2) between satellite LST and ground temperature was calculated using simple linear regression. Spatial correspondence was evaluated visually. A conceptual explanation was developed to interpret the mismatch between spatial and numerical relationships.

3 RESULTS

3.1 Temperature Maps

Landsat-derived LST values ranged from 31°C to 38°C (Figure 3 left), while measured ground temperatures ranged from 15°C to 95°C from dataset (interpolated in Figure 3 right). Despite this magnitude difference, elevated LST zones correspond spatially to interpolated shallow ground temperature areas. Note that the color scale range in Figures 3 left and right were intentionally adjusted to emphasize the relative spatial distribution of thermal anomalies. A uniform scale range for both figures would have suppressed the contrast and made the spatial patterns less discernible.

It should be noted that the higher interpolated temperature values appearing outside the measured area are artifacts of the interpolation algorithm, which extrapolates beyond the sampled points. Consequently, these values do not represent actual field conditions and should not be directly compared with the Landsat LST pixel data. The predicted values may not follow the trend of the nearest sampled points, for instance, as observed in the northeastern part of the map in Figure 3b, where areas beyond the last low-value sampling points display artificially elevated temperatures.

The scatterplot (Figure 4) shows weak correlation ($R^2 \approx 0.04$), suggesting very low correlation. Nevertheless, spatial alignment of high-temperature areas depicted at Figure 3 previously indicates a consistent qualitative relationship between both datasets.

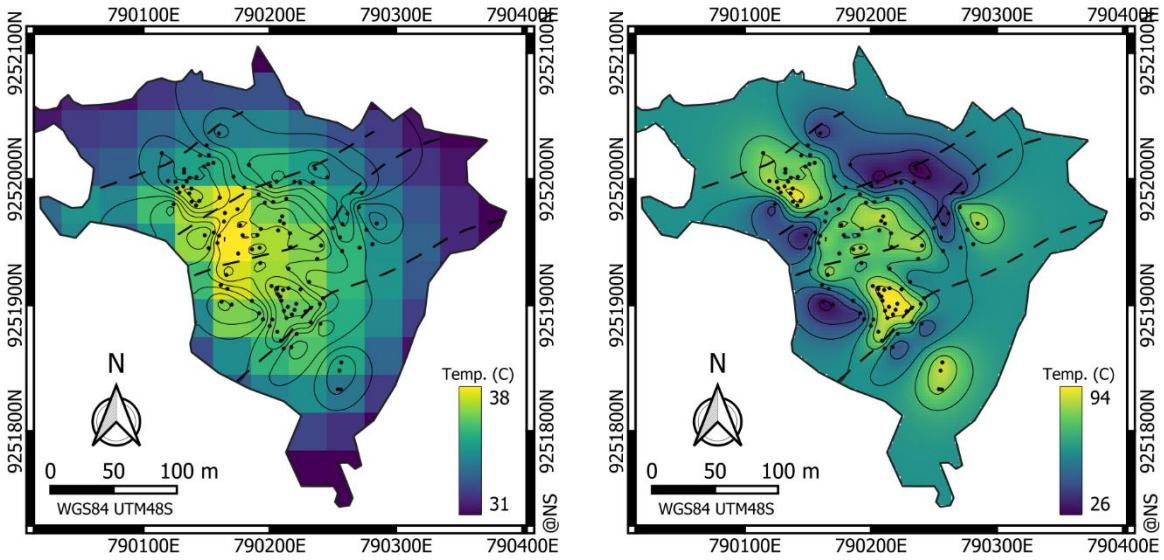


Figure 3. Landsat LST map (left) and Interpolated shallow ground temperature map (right). (Color scale ranges differ between Figures left and right to better highlight thermal anomalies.)

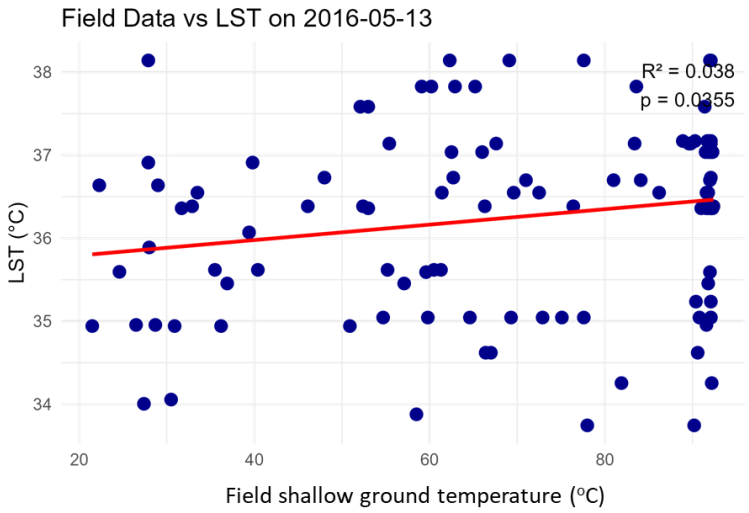


Figure 4. Scatterplot of Landsat LST versus measured shallow ground temperature.

3.2 Temperature Difference Map

To further examine the relationship between satellite and ground temperatures, a difference map was generated by subtracting interpolated ground temperature data from Landsat-derived LST. The field temperature map was first downscaled to match the Landsat pixel resolution (30 m) using bilinear interpolation.

Figure 5 illustrates (left) the downscaled ground temperature map and (right) the difference (LST – Ground) map. The overall pattern shows that Landsat LST values are consistently lower than shallow ground temperatures, with temperature differences ranging from approximately -4°C to -41°C.

Interestingly, the difference tends to increase at locations of higher ground temperature anomalies. This suggests that LST underestimates the actual near-surface thermal condition more strongly where surface heat flux is greatest.

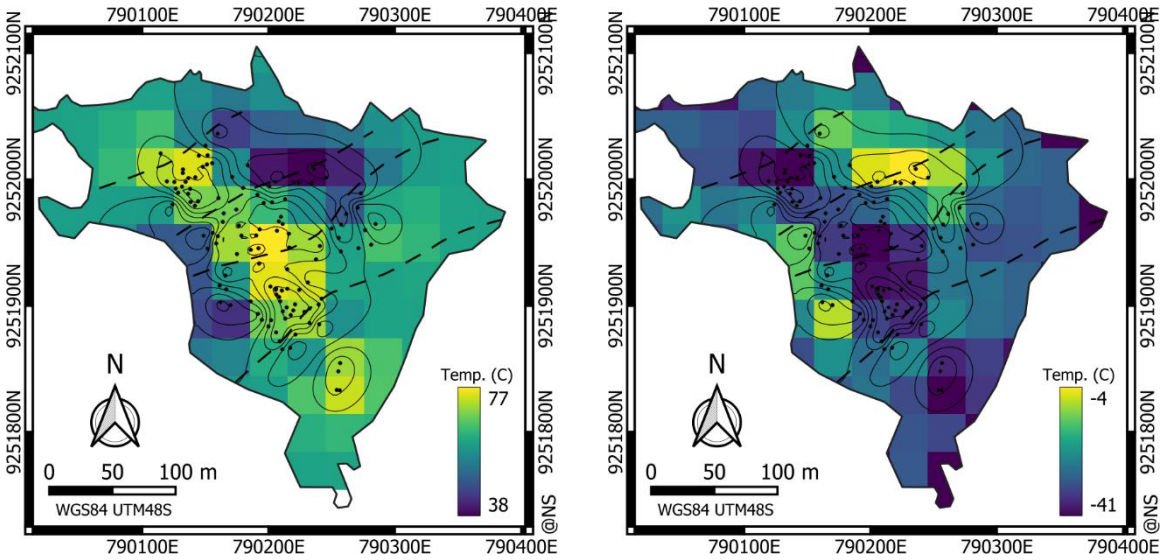


Figure 5. (Left) Downscaled ground temperature map; (Right) Temperature difference (LST – Ground) map.

3.3 Alteration Patterns

The spatial distribution of alteration indices is shown in the clay index map (Figure 6, left) and the silica index map (Figure 6, right). The clay index exhibits lower values in areas corresponding to higher surface temperatures, suggesting that clay-rich materials are less abundant or altered in zones of thermal anomalies. This pattern indicates a potential negative correlation between clay alteration and temperature anomalies in the study area. The silica index, in contrast, shows relatively higher values in the high-temperature zones, although the values slightly decrease and are smeared toward the northeast. This suggests that silica alteration is more pronounced in thermally active areas but exhibits spatial dispersal, possibly influenced by structural controls or surface processes.

Overall, the clay and silica index maps provide complementary insights into the alteration patterns, and their spatial correspondence with temperature anomalies highlights areas of potential geothermal activity.

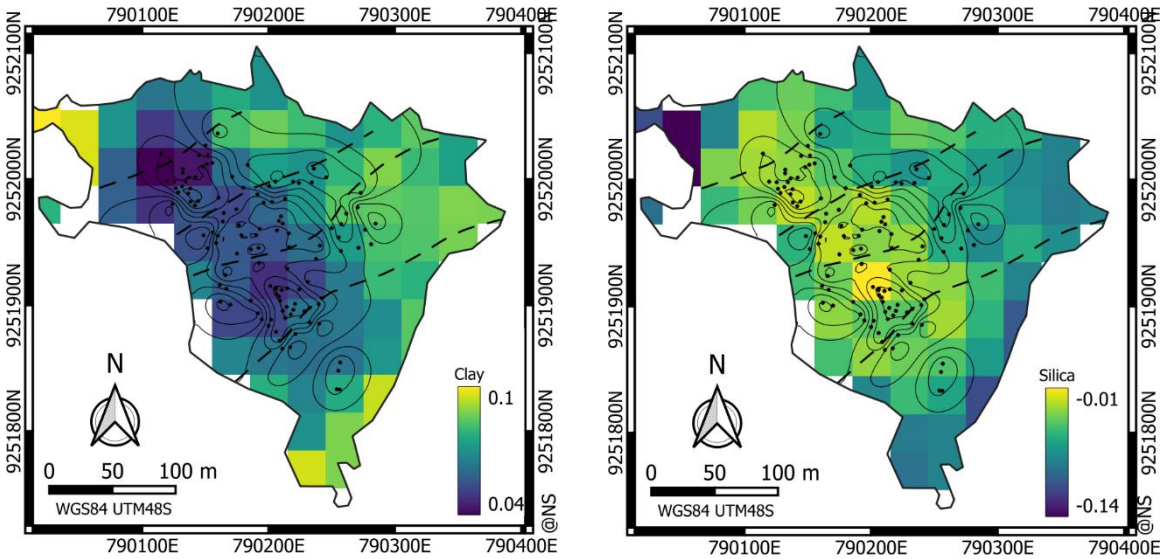


Figure 6. (Left) Clay Alteration Index; (Right) Silica Alteration Index.

4 DISCUSSION

4.1 Causes of Weak Correlation

The poor correlation mainly arises from (1) Spatial-scale mismatch: each Landsat TIR pixel (100 m, resampled into 30 m) integrates multiple land-cover conditions even in barren crater setting, while field measurements represent a few centimeters and (2) Depth difference: ground measurements reflect subsurface conductive heat

at 25–50 cm depth, whereas LST represents instantaneous surface emission influenced by albedo and emissivity.

4.2 Interpreting Visual Agreement

Despite poor statistics (low correlation coefficient, R), the spatial alignment between high LST zones and geothermal features confirms that LST retains qualitative value. It effectively delineates relative hot zones but cannot predict absolute subsurface temperatures. That said, when the NE–SW structural features mapped from field observations are overlaid (Figure 3, left), they seem to roughly correspond to the transition boundaries between high anomaly zones on the LST map. This apparent correspondence is, however, qualitative and should be regarded as a tentative observation given the coarse pixel resolution of the LST data.

4.3 Temperature Difference Pattern

The difference analysis reveals that Landsat LST systematically underestimates ground temperatures, with the largest discrepancies occurring in areas of high geothermal activity. Several factors may contribute to this pattern:

1. **Surface–subsurface decoupling:**
   High ground temperatures often originate from subsurface conductive or convective processes. The LST signal, representing instantaneous surface radiation, may cool rapidly due to wind, moisture, or emissivity variation, thus underestimating true thermal intensity (Kuenzer & Dech, 2013; Li et al., 2013).

2. **Thermal emissivity and mixing effects:**
   Despite a relatively homogeneous crater surface, the 100 m Landsat pixel inevitably mixes radiance from any sub-pixel features present, such as hot spots, dry soils, and wet altered zones. This integration of radiance across different surface types is a fundamental characteristic of the sensor's spatial resolution and can reduce the apparent radiance temperature compared to the higher temperatures measured at specific ground locations (Barsi et al., 2014).

3. **Atmospheric and temporal differences:**
   Landsat captures conditions at a single time (morning local time (U.S. Geological Survey (n.d.))), whereas field temperatures integrate accumulated subsurface heat. Temporal offset and atmospheric attenuation further suppress apparent surface temperature (Urban et al., 2003).

4.4 Thermal and Mineralogical Correlations

The observed inverse relationship between the clay alteration index and surface temperature suggests that areas with higher thermal anomalies are associated with lower clay content. This pattern may indicate that clay-rich zones are less prevalent or have undergone alteration processes that reduce their thermal emissivity. Such findings are consistent with previous studies where clay minerals, particularly those associated with hydrothermal alteration, exhibit distinct spectral signatures in the shortwave infrared (SWIR) bands of Landsat imagery (Testa et al., 2018).

Conversely, the silica index map reveals higher values in regions with elevated temperatures, albeit with a slight decrease and spatial dispersion toward the northeast. This distribution implies that silica-rich alteration zones are more prevalent in thermally active areas, aligning with the known association between silica alteration and hydrothermal systems. The northeastward spread could be attributed to geological factors such as faulting or fluid migration pathways that influence the extent of alteration zones.

4.5 Implications

LST is best applied for relative anomaly detection during reconnaissance surveys. The temperature-difference analysis shows that Landsat LST values are systematically lower than measured ground temperatures, with larger discrepancies over zones of stronger geothermal activity. This underestimation indicates that satellite-derived thermal data tend to smooth or dampen extreme surface temperatures, making them more suitable for identifying *relative* rather than *absolute* thermal anomalies.

In the nearly vegetation-free Kawah Domas crater, the apparent visual-spatial coherence between LST and field patterns may be partly related to the reduced influence of surface interference. In more vegetated or compositionally heterogeneous terrains, complementary use of NDVI, geological, and structural data is recommended to refine thermal anomaly interpretation and mitigate emissivity and mixed-pixel effects.

The spatial distribution of the alteration indices relative to temperature anomalies underscores the potential of using remote sensing data to identify areas of hydrothermal alteration. The presence of silica-rich zones in high-temperature regions supports the hypothesis of active hydrothermal systems, as silica is commonly associated with such environments (Pour & Hashim, 2015).

Additionally, the observed patterns suggest that the thermal anomalies and alteration indices could serve as proxies for identifying prospective areas for further geological exploration. Integrating these remote sensing-derived indices with geological and geophysical data could enhance the accuracy of mapping hydrothermal alteration zones and understanding their spatial distribution.

4.6 Limitations

While the study provides valuable insights, it is important to recognize the inherent limitations of the data. The spatial resolution of Landsat imagery, although appropriate for regional-scale analysis, may not capture fine-scale variations in alteration zones. By acknowledging this limitation, interpretations can be adjusted accordingly, focusing on patterns and trends that are meaningful at the available resolution. This approach allows us to maximize the insights that can be reliably derived from the data while remaining cautious about over-interpreting small-scale features.

Furthermore, the interpretation of alteration indices should be understood in the context of exploration-stage objectives. While detailed laboratory or field validation can provide additional certainty, the primary aim at this stage is to maximize the information that can be reliably extracted from remote sensing data. By carefully analyzing spatial patterns, correlations with temperature anomalies, and relative differences between clay and silica indices, we can identify promising areas for follow-up exploration and make informed decisions without overextending interpretations beyond the data's resolution and scope.

5 CONCLUSIONS

This study integrated Landsat-derived Land Surface Temperature (LST) with field-measured subsurface temperatures and SWIR-based alteration indices to assess thermal anomalies and surface mineralogy in the study area. The analysis demonstrates the following key findings:

1. Temperature anomalies: LST and ground-based measurements revealed distinct high-temperature zones, highlighting areas of potential geothermal activity. Temperature-difference maps (LST – Ground) illustrated the spatial distribution and magnitude of discrepancies between satellite and field observations, which are expected due to differences in spatial resolution and surface conditions.

2. Clay and silica alteration patterns: The SWIR-based indices provided valuable insights into surface mineralogy. The clay index exhibited lower values in high-temperature areas, suggesting reduced clay presence or alteration in thermally active zones. The silica index showed relatively higher values in the same zones, with slight northeastward dispersion, indicating that silica-rich alteration is more prevalent and spatially extensive in thermally anomalous areas.

3. Exploration-stage interpretation: By combining LST and SWIR indices, the study maximized the information that can be extracted at the exploration stage. Despite inherent limitations in spatial resolution, the integrated maps of temperature and alteration indices provide meaningful guidance for identifying promising areas for further investigation.

Overall, the combination of thermal and mineralogical remote sensing indicators offers a practical approach for early-stage geothermal exploration, enabling the identification of zones with potential hydrothermal alteration and informing subsequent field targeting.

REFERENCES

Augusty, D. G., Bagaskara, M. F., & Oktaviani, A. D. (2022). Analisis potensi panas bumi pada daerah G. Karang, Banten, menggunakan metode penginderaan jauh [Analysis of geothermal potential in the Mount Karang area, Banten, using the remote sensing method]. Jurnal Teknik Geologi: Jurnal Ilmu Pengetahuan Dan Teknologi, 5(2).

Barsi, J. A., Schott, J. R., Hook, S. J., Raqueno, N. G., Markham, B. L., & Radocinski, R. G. (2014). Landsat-8 Thermal Infrared Sensor (TIRS) vicarious radiometric calibration. Remote Sensing, 6(11), 11607–11626. https://doi.org/10.3390/rs61111607

Dewanto, B. G., Hadmoko, D. S., Ramadhani, N. F., & Julius, A. M. (2025). Multitemporal satellite images for monitoring the volcanic activities and geothermal potential of Ternate Island's Gamalama Volcano, Indonesia's densest active volcanic island. Remote Sensing Applications: Society and Environment, 38, 101555. https://doi.org/10.1016/j.rsase.2025.101555

Fathya, A. B., Nugraha, H. S., Ranti, A. G., & Wahyuningsih, R. (2023). Analysis of anomaly land surface temperature using Landsat 8 satellite imagery to identify geothermal prospect of Mount Sirung in Alor Regency, East Nusa Tenggara Province. Buletin Sumber Daya Geologi, 18(1), 37–54. https://doi.org/10.47599/bsdg.v18i1.367

Hidayat, M. R., Marin, J., Abdurrahman, R. B., Devienna, S. N., & Fatimah, I. N. (2023). Land surface temperature (LST) and fault fracture density (FFD) analysis in Bukit Kili-Gunung Talang geothermal area, West Sumatra. Journal of Aceh Physics Society, 12(2), 39–48.

Jiménez-Muñoz, J. C., & Sobrino, J. A. (2003). A generalized single-channel method for retrieving land surface temperature from remote sensing data. Journal of Geophysical Research: Atmospheres, 108(D22), 4688. https://doi.org/10.1029/2003JD003480

Kuenzer, C., & Dech, S. (Eds.). (2013). Thermal infrared remote sensing: Sensors, methods, applications. Springer. https://doi.org/10.1007/978-94-007-6639-6

Li, Z., Tang, B., Wu, H., Ren, H., Yan, G., Wan, Z., Trigo, I. F., & Sobrino, J. A. (2013). Satellite-derived land surface temperature: Current status and perspectives. Remote Sensing of Environment, 131, 14–37. https://doi.org/10.1016/j.rse.2012.12.008

Ninomiya, Y. (2003). A stabilized vegetation index and several mineralogic indices defined for ASTER VNIR and SWIR data. In IGARSS 2003: 2003 IEEE International Geoscience and Remote Sensing Symposium. Proceedings (Vol. 3, pp. 1552-1554). IEEE. https://doi.org/10.1109/IGARSS.2003.1294172

Nugraha, H. S., Permana, L. A., & Sukaesih. (2021). Landsat 8 and DEMNAS images analyses to identify geothermal prospect in Central Aceh Regency, Aceh Province. Buletin Sumber Daya Geologi, 16(3). https://doi.org/10.47599/bsdg.v16i3.322

Pour, A. B., & Hashim, M. (2015). Hydrothermal alteration mapping from Landsat-8 data, Sar Cheshmeh copper mining district, south-eastern Islamic Republic of Iran. Journal of Taibah University for Science, 9(2), 155–166. https://doi.org/10.1016/j.jtusci.2014.11.008

Sabins, F.F., 1999. Remote sensing for mineral exploration. Ore Geol. Rev. 14, 157–183. https://doi.org/10.1016/S0169-1368(99)00007-4

Testa, F. J., Villanueva, C., Cooke, D. R., & Zhang, L. (2018). Lithological and hydrothermal alteration mapping of epithermal, porphyry and tourmaline breccia districts in the Argentine Andes using ASTER imagery. Remote Sensing, 10(2), 203. https://doi.org/10.3390/rs10020203

Urban, M., Eberle, J., Hüttich, C., Schmullius, C., & Herold, M. (2013). Comparison of satellite-derived land surface temperature and air temperature from meteorological stations on the pan-Arctic scale. Remote Sensing, 5(5), 2348–2367. https://doi.org/10.3390/rs5052348

U.S. Geological Survey. (2023, October 26). Landsat Collection 2 Level-2 science products. Landsat Missions. https://www.usgs.gov/landsat-missions/landsat-collection-2-level-2-science-products

U.S. Geological Survey. (n.d.). How can I find the acquisition time for a Landsat scene? Retrieved October 17, 2025, from https://www.usgs.gov/faqs/how-can-i-find-acquisition-time-a-landsat-scene